

A time-orbiting potential chip trap for cold atoms

C. A. Sackett*

Department of Physics, University of Virginia, Charlottesville, Virginia 22904, USA

J. C. Stickney

Space Dynamics Laboratory, North Logan, UT 84341, USA

(Dated: February 2, 2023)

We present a design for an atom chip trap that uses the time-orbiting potential technique. The design offers several advantages compared to other chip-trap methods. It uses a simple crossed-wire pattern on the chip, along with a rotating bias field. The trap is naturally cylindrically symmetric and can be made spherically symmetric. Loading from a magneto-optical trap is facilitated because the trap can be positioned an arbitrary distance from the chip. The fields can be modified to provide a gradient for support against gravity, and the three-dimensional trap can be adiabatically transformed into a two-dimensional guide.

Over the past two decades, atom chips have become a critical technology for ultracold atom science [1–3]. An atom chip consists of small current-carrying wires patterned onto a planar substrate. Atoms near the wires experience very large magnetic field gradients, which enables the production of tightly confining magnetic traps with relatively low electrical power consumption. Atom chips are used in many research laboratories, they are the basis for commercial ultra-cold atom systems [4, 5], and they have enabled the production of cold atoms in microgravity [6, 7].

Most implementations of an atom chip use the Ioffe-Pritchard trap configuration [8]. This can be produced, for instance, by a Z-shaped wire as in Fig. 1(a) [1]. This “Z trap” is suitable for evaporative cooling and has been used to produce quantum degenerate gases in many experiments. It does, however, have some drawbacks that our design aims to redress. First, if the center segment of the Z has length $2a$, then the potential minimum cannot be located further than $1.2a$ from the chip surface due to an inflection point in the field curvature [9]. This constrains the ability to load atoms directly from a Magneto-Optical Trap (MOT) into the Z trap, since the MOT is typically located several mm from the surface. Second, when the atoms are moved close to the chip to produce a tight trap for rapid cooling, the confinement along the wire direction is relatively weak, leading to a highly asymmetric trap and a reduction in cooling efficiency. Adding additional wires to the chip can to some degree alleviate these drawbacks [1], but it is generically difficult to produce a trap that is tightly confining, approximately symmetric, and with a chip distance that is continuously variable up to several mm.

A different technique used for magnetic trapping of atom is the Time-Orbiting Potential (TOP) [10]. Here a uniformly rotating bias field is combined with a static or oscillating gradient field to produce a time-averaged potential that is approximately harmonic. TOP traps are

generally less sensitive to static or low-frequency environmental field noise, since the time average of the atomic moments are zero. TOP traps also permit the use of ac electronic techniques like transformers and resonant circuits, which can efficiently generate high currents in many cases. TOP traps are typically produced using macroscopic coils, although the technique has sometimes been applied with atom chips for special uses [11].

We propose here to combine the atom-chip and TOP-trap ideas in a simple way that maintains the utility of each. The chip implementation uses the cross-wire configuration shown in Fig. 1(b), along with uniform bias fields parallel to the chip plane. Notably, this configuration has no geometric parameter analogous to a of the Z trap, since the cross wires can be arbitrarily long. The concept of this trap is slightly different from that of a conventional TOP trap: Consider first a dc current passing through the x wire of the cross in Fig. 1(b). Adding a bias field β in the $+y$ direction produces a line of field zeros running above the x axis. An additional bias field component γ along x converts this line into a harmonic

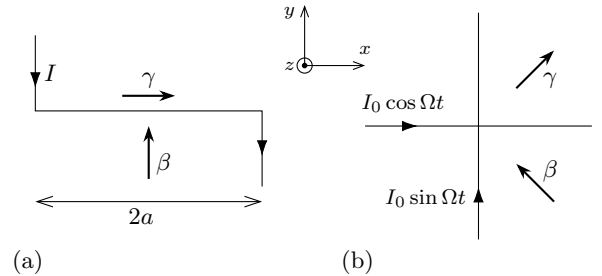


FIG. 1. Atom chip configurations. Thin lines represent wires on the chip carrying current I , and thicker arrows represent uniform field components. (a) Ioffe-Pritchard “Z trap” configuration. The β field sets the distance of the trap from the chip, while the γ field provides a non-zero bias at the trap center. (b) Cross trap configuration. The β and γ fields play similar roles as in the Z trap, but here the bias fields rotate in sync with the oscillating wire currents. The diagram shows the field and current directions when $\Omega t = \pi/4$.

* sackett@virginia.edu

minimum, which provides confinement along the y and z directions but a uniform potential along x . To generate three-dimensional confinement, the cross wires are instead driven with oscillating currents $\cos \Omega t$ and $\sin \Omega t$ while the bias fields rotate in sync. The shape of the net field is not constant in time, but it approximates a rotating two-dimensional trap. As long as Ω is sufficiently large, the atoms experience the time-averaged field, which produces a three-dimensional trap.

To analyze the system, we set the coordinate origin at the center of the cross. The fields involved can be expressed as

$$\begin{aligned} \mathbf{B}(t) = & \frac{\mu_0 I_0}{2\pi} \left[\frac{y\hat{z} - z\hat{y}}{y^2 + z^2} \cos \Omega t + \frac{z\hat{x} - x\hat{z}}{x^2 + z^2} \sin \Omega t \right] \\ & + \beta (\hat{y} \cos \Omega t - \hat{x} \sin \Omega t) \\ & + \gamma (\hat{x} \cos \Omega t + \hat{y} \sin \Omega t). \end{aligned} \quad (1)$$

The first line gives the field from the chip wires, which are assumed to be long and thin. Here I_0 is the current amplitude, μ_0 is the magnetic constant, and Ω is the time-orbiting frequency. The second line gives the bias component perpendicular to the wires, with amplitude β . The trap center will occur where the chip field and the β field cancel, at

$$z = z_0 \equiv \frac{\mu_0 I_0}{2\pi\beta}. \quad (2)$$

We use z_0 and β as independent variables in the following: z_0 because it is experimentally significant, and β because it leads to relatively simple formulas. We thus take implicitly that $I_0 = 2\pi\beta z_0/\mu_0$. The third line in Eq. (1) is the bias component γ that provides a non-zero trap minimum. Although the decomposition shown here is convenient for analysis, the total bias can be implemented as a single rotating field

$$\mathbf{B}_{\text{bias}}(t) = \sqrt{\beta^2 + \gamma^2} [\hat{x} \cos(\Omega t + \theta) + \hat{y} \sin(\Omega t + \theta)] \quad (3)$$

with phase $\theta = \tan^{-1}(\beta/\gamma)$ relative to the chip currents.

To characterize the trap, we Taylor expand the field components around the trap center, taking $\zeta = z - z_0$. The field magnitude is

$$\begin{aligned} B(t) = & \sqrt{B_x^2 + B_y^2 + B_z^2} \\ \approx & \gamma + \frac{\beta^2}{2\gamma z_0^2} (x^2 \cos^2 \Omega t + y^2 \sin^2 \Omega t + \zeta^2) \\ & - \frac{2\beta}{z_0^2} (x^2 + xy - y^2) \sin \Omega t \cos \Omega t \end{aligned} \quad (4)$$

to second order in the coordinates. Time averaging yields the effective potential

$$V(\mathbf{r}) = \mu \langle B \rangle = \mu \gamma + \frac{\mu \beta^2}{4\gamma z_0^2} (\rho^2 + 2\zeta^2) \quad (5)$$

where μ is the magnetic moment of the atomic state and $\rho^2 = x^2 + y^2$. The potential is confining and cylindrically

symmetric, with harmonic oscillation frequencies

$$\omega_\rho = \sqrt{\frac{\mu\beta^2}{2m\gamma z_0^2}}, \quad \omega_z = \sqrt{2}\omega_\rho \quad (6)$$

for atomic mass m .

In comparison, a Z trap with chip distance $z_0 \ll a$ has oscillation frequencies

$$\omega_y^{(Z)} = \omega_z^{(Z)} = \sqrt{\frac{\mu\beta^2}{m\gamma z_0^2}}, \quad \omega_x^{(Z)} = \frac{2z_0^2}{a^2} \omega_z^{(Z)} \quad (7)$$

where β and γ are again the transverse and longitudinal bias fields. Here we see that the net curvature $\omega_x^2 + \omega_y^2 + \omega_z^2$ is the same for both traps (neglecting z_0^4/a^4), while $(\omega_x \omega_y \omega_z)^{1/3}$ is larger in the cross trap by a factor of $(a/z_0)^{2/3}$. The density of the trapped atom cloud is set by the geometric mean, making it most relevant for efficient evaporative cooling and many other applications.

Figure 2 compares the numerically calculated trap potential to the harmonic approximation derived above. As to be expected, the confining potential is harmonic only very near the trap center. It is possible to extend the analytical calculation to higher orders and extract the leading anharmonic terms. With the aid of symbolic math software, we find the fourth-order expansion

$$\begin{aligned} \langle B \rangle \approx & \gamma + \frac{\beta^2}{4\gamma z_0^2} \left\{ \rho^2 + 2z^2 - \frac{2}{z_0} (\rho^2 z + z^3) \right. \\ & - \frac{1}{16z_0^2} \left[\left(20 + \frac{3\beta^2}{\gamma^2} \right) \rho^4 + \left(28 + \frac{3\beta^2}{\gamma^2} \right) x^2 y^2 \right. \\ & + \frac{8\beta^2}{\gamma^2} (xy^3 - x^3 y) + 8 \left(\frac{\beta^2}{\gamma^2} - 4 \right) \rho^2 z^2 \\ & \left. \left. + 8 \left(\frac{\beta^2}{\gamma^2} - 12 \right) z^4 \right] \right\}, \end{aligned} \quad (8)$$

The anharmonic terms become important for coordinate excursions on the order of z_0 or $\gamma z_0/\beta$, whichever is smaller.

The preceding results confirm that there is no intrinsic geometrical length scale for the cross chip TOP trap, since z_0 can be made as small or large as desired. In practice, however, the range of z_0 will be constrained on the large side by the finite length L of the cross wires. The impact of this will depend on how current is delivered to the chip. If the current enters via long lead wires perpendicular to the chip, the dominant effect is that the leads contribute a field parallel to the β field, which moves the trap minimum closer to the chip and makes the trap more confining. If β is reduced to keep z_0 constant, there is a modest reduction in the confinement frequencies. For $L/z_0 > 4$, the reduction is less than 10%. The range of z_0 is limited on the small side by the width w of the chip wires, since the thin-wire approximation will fail. If the wires are modeled as flat strips, we find that as z_0 is reduced, the trap minimum moves closer to the chip than

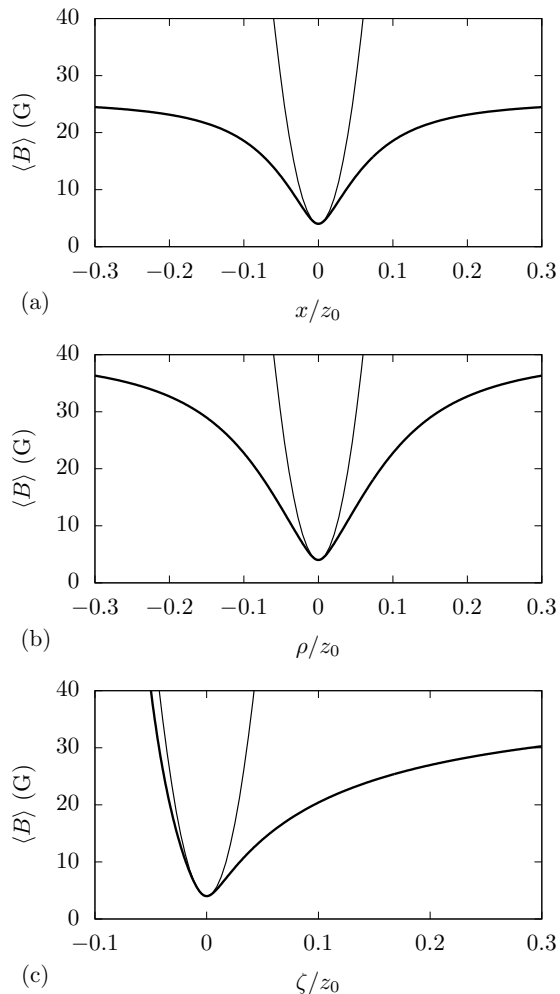


FIG. 2. Trapping potential for cross trap, for parameters $I_0 = 20$ A, $\beta = 40$ G, and $\gamma = 4$ G. These provide a potential minimum at $z_0 = 1$ mm. The heavier curves show the time-averaged magnetic field magnitude and the lighter curves are the quadratic approximation of Eq. (5). (a) Plot of the average field and quadratic approximation along the x axis at $z = z_0$. (b) Plot of the average field and quadratic approximation along the line $x = y$, for $\rho = \sqrt{x^2 + y^2}$ and with $z = z_0$. (c) Plot of the average field and quadratic approximation along the z axis, with $\zeta = z - z_0$.

z_0 and the confinement becomes weaker. Both $\Delta z/z_0$ and $\Delta\omega/\omega$ remain less than 10% down to $z_0 \approx w$.

Unlike a conventional TOP trap [10], the cross chip trap has no field zero, so there is no “circle of death” limiting the trap depth. Instead the depth D is set by the time-averaged field above the wires far from the origin. The depth cannot be expressed as a simple analytic function, but it is of order $D_0 \equiv \sqrt{\beta^2 + \gamma^2} - \gamma$. A numerical calculation of the depth is shown in Fig. 3.

The cross trap can be modified in a simple way by altering the phase of the bias fields, such that for instance the γ field becomes $\gamma[\hat{x} \cos(\Omega t + \phi) + \hat{y} \sin(\Omega t + \phi)]$. In terms of a single bias field as in Eq. (3), the magnitude

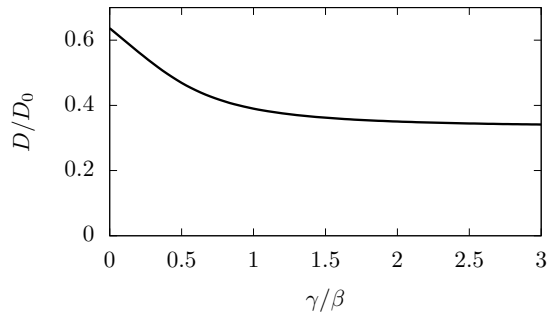


FIG. 3. Trap depth D for the cross trap, where $D_0 = \sqrt{\beta^2 + \gamma^2} - \gamma$. For large γ/β , the depth approaches $D_0/3 = \beta^2/6\gamma$, and for $\gamma/\beta \rightarrow 0$, the depth approaches $2D_0/\pi = 2\beta/\pi$.

is $\sqrt{\beta^2 + \gamma^2 + 2\gamma\beta \sin \phi}$ and the phase is $\theta = \tan^{-1}[(\beta + \gamma \sin \phi)/(\gamma \cos \phi)]$. Re-evaluating the time-averaged field to second order yields

$$\begin{aligned} \langle B \rangle = & \gamma + \beta \sin \phi \frac{\zeta}{z_0} + \left(\frac{\beta^2}{4\gamma} + \frac{1}{2} \beta \sin \phi \right) \frac{\rho^2}{z_0^2} \\ & + \left(\frac{\beta^2}{2\gamma} \cos^2 \phi - \beta \sin \phi \right) \frac{\zeta^2}{z_0^2}. \end{aligned} \quad (9)$$

The term linear in ζ can be used to compensate for gravity in a weak trap.

Alternatively, we can model a case where the γ field rotation rate is different from Ω , by taking $\phi = \Delta t$ for constant Δ . We then have $\langle \sin \phi \rangle \rightarrow 0$ and $\langle \cos^2 \phi \rangle \rightarrow 1/2$, leading to a spherically symmetric trap with isotropic frequency $\omega^2 = \mu\beta^2/(2m\gamma z_0^2)$. This could be achieved with $\Delta = -\Omega$, which corresponds to a static field γ pointing in any direction parallel to the chip. Use of a static field, however, would re-introduce sensitivity to dc background fields.

As an example of a potential application, we describe an atom chip capable of capturing atoms from a MOT located several mm from the chip, and then compressing the atoms to a trap with confinement frequencies above 1 kHz for evaporative cooling. We consider a chip fabricated from 100- μm thick direct-bonded copper on an aluminum-nitride substrate [12]. The side of the chip facing the atoms is patterned to produce cross wires that are 100 μm wide. The opposite side is has a matching cross pattern with wires 3 mm wide. Take the chip size L to be 3 cm and the total chip thickness to be 1 mm. The wider cross is used to produce a distant trap for loading. Using a current amplitude of $I_0 = 75$ A, bias fields $\beta = 20$ G, $\gamma = 2$ G, and a phase $\phi = 0.85$ rad, the resulting trap is 7 mm from the chip. Rubidium atoms will be supported against gravity with confinement frequencies $\omega_\rho \approx 2\pi \times 18$ Hz and $\omega_z \approx 2\pi \times 13$ Hz, and a trap depth of 12 G ≈ 800 μK . These are appropriate values for efficient loading from a MOT [13]. The total power consumption on the chip is about 10 W, which is well within the capacity of this type of substrate [12].

Once the trap is loaded, current through the wide cross can be adiabatically decreased, which reduces z_0 and compresses the trap. Once the atoms are within a few mm of the chip, the current is adiabatically shunted to the thin cross, supporting smaller z_0 . A current of 5 A and bias fields $\beta = 40$ G, $\gamma = 2$ G would generate a trap 0.25 mm from the chip surface with $\omega_\rho \approx 2\pi \times 1$ kHz and $\omega_z \approx 2\pi \times 1.4$ kHz. This makes a suitable trap for rapid evaporative cooling. Power dissipation on the chip would be about 1 W. A different approach to supporting a wide range of z_0 values using a single-layer chip is to use tapered wires whose widths decrease as they approach the cross center.

A final noteworthy feature of the cross TOP configuration is that the three-dimensional trap can be converted to a two-dimensional guide. This configuration could be useful for applications involving atom transport, including atom interferometry [14, 15]. It is achieved by reducing the current through one of the wires to zero along with the corresponding β field component. For a guide along the x axis, the resulting field is

$$\mathbf{B}(t) = \beta \cos \Omega t \left[\hat{y} + \frac{z_0(y\hat{z} - z\hat{y})}{y^2 + z^2} \right] + \gamma (\hat{x} \cos \Omega t + \hat{y} \sin \Omega t), \quad (10)$$

with still $z_0 = \mu_0 I_0 / 2\pi\beta$ for chip current amplitude I_0 . The time-averaged field has the form

$$\langle B \rangle = \gamma + \frac{\beta^2}{4\gamma z_0^2} \left(y^2 + \frac{3}{4}\zeta^2 \right) \quad (11)$$

with $\zeta = z - z_0$, and thus provides harmonic confinement with $\omega_y^2 = \mu\beta^2 / (2\gamma z_0^2)$ and $\omega_z = (\sqrt{3}/2)\omega_y$. For example, if $\beta = 40$ G, $\gamma = 2$ G and $I = 5$ A as in the trap previously considered, the guide distance remains at 0.25 mm and the confinement frequencies for ^{87}Rb are about 1 kHz and 800 Hz. Power dissipation on the chip is reduced

by a factor of two compared to the equivalent trap. The guide potential can similarly be modified by introducing a phase ϕ to the γ field as in Eq. (9), resulting in

$$\langle B \rangle = \gamma + \frac{1}{2}\beta \sin \phi \frac{\zeta}{z_0} + \left(\frac{\beta^2}{4\gamma} + \frac{1}{2}\beta \sin \phi \right) \frac{y^2}{z_0^2} + \left[\frac{\beta^2}{16\gamma} (1 + 2\cos^2 \phi) - \frac{1}{2}\beta \sin \phi \right] \frac{\zeta^2}{z_0^2}. \quad (12)$$

In summary, the cross TOP trap provides a chip-based trap with confinement comparable or better than that of typical Ioffe-Pritchard configurations. The confinement is naturally cylindrically symmetric and can be readily modified to be spherically symmetric and to provide support against gravity. The trap center can be positioned further from the chip than possible with conventional approaches, and the same chip geometry can provide a two-dimensional atom guide. We expect that these features will make the cross TOP useful for a variety of applications. One example is the atomic Sagnac interferometer of [16], where the cross trap could significantly simplify the apparatus and allow faster production of Bose condensates, thus increasing the sensing bandwidth. For this purpose, the cylindrical symmetry of the trap is critical. We are also exploring how the approach could be extended to produce bias fields with the chip itself, and thereby remove the need for external coils. By such means, we hope this method will facilitate the use of ultracold atom techniques in practical applications.

ACKNOWLEDGMENTS

This work was supported by DARPA (Award No. FA9453-19-1-0007). The authors thank M. Beydler, E. Imhof, B. Kasch, E. Moan, and E. Salim for helpful advice and conversations.

-
- [1] J. Reichel, *Appl. Phys. B* **74**, 469 (2002).
[2] J. Reichel and V. Vuletic, eds., *Atom Chips* (Wiley VCH, Weinheim, 2011).
[3] M. Keil, O. Amit, S. Zhou, D. Groswasser, Y. Japha, and R. Folman, **63**, 1840 (2016).
[4] S. Du, M. B. Squires, Y. Imai, L. Czaia, R. A. Saravanan, V. Bright, J. Reichel, T. W. Hänsch, and D. Z. Anderson, *Phys. Rev. A* **70**, 053606 (2004).
[5] D. M. Farkas, E. A. Salim, and J. Ramirez-Serrano, Production of rubidium Bose-Einstein condensates at a 1 Hz rate (2014), arXiv:1403.4641 [physics.atom-ph].
[6] A. Vogel, M. Schmidt, K. Sengstock, K. Bongs, W. Lewoczko, T. Schuldt, A. Peters, T. V. Zoest, W. Ertmer, E. Rasel, T. Steinmetz, J. Reichel, T. Könemann, W. Brinkmann, E. Göklü, C. Lämmerzahl, H. Dittus, G. Nandi, W. Schleich, and R. Walser, *App. Phys. B* **84**, 663 (2006).
[7] D. C. Aveline, J. R. Williams, E. R. Elliott, C. Dutenhof-fer, J. R. Kellogg, J. M. Kohel, N. E. Lay, K. Oudrhiri, R. F. Shotwell, N. Yu, and R. J. Thompson, **582**, 193 (2020).
[8] W. Ketterle and D. E. Pritchard, *Appl. Phys. B* **54**, 403 (1992).
[9] C. A. Sackett, T. C. Lam, J. C. Stickney, and J. H. Burke, *Micrograv. Sci. and Tech.* <https://doi.org/10.1007/s12217-017-9584-3> (2017), <https://doi.org/10.1007/s12217-017-9584-3>.
[10] W. Petrich, M. H. Anderson, J. R. Ensher, and E. A. Cornell, *Phys. Rev. Lett.* **74**, 3352 (1995).
[11] S. Gupta, K. W. Murch, K. L. Moore, T. P. Purdy, and D. M. Stamper-Kurn, *Phys. Rev. Lett.* **95**, 143201 (2005).
[12] M. B. Squires, J. A. Stickney, E. J. Carlson, P. M. Baker, W. R. Buchwald, S. Wentzell, and S. M. Miller, *Rev. Sci. Instrum.* **82**, 023101 (2011).
[13] M. B. Squires, S. E. Olson, B. Kasch, J. A. Stickney, C. J. Erickson, J. A. R. Crow, E. J. Carlson, and J. H. Burke,

- Appl. Phys. Lett. **109**, 264101 (2016).
- [14] D. Müller, D. Z. Anderson, R. J. Grow, P. D. D. Schwindt, and E. A. Cornell, Phys. Rev. Lett. **83**, 5194 (1999).
- [15] Y. J. Wang, D. Z. Anderson, V. M. Bright, E. A. Cornell, Q. Diot, T. Kishimoto, M. Prentiss, R. A. Saravanan, S. R. Segal, and S. Wu, Phys. Rev. Lett. **94**, 090405 (2005).
- [16] E. R. Moan, R. A. Horne, T. Arpornthip, Z. Luo, A. J. Fallon, S. J. Berl, and C. A. Sackett, Phys. Rev. Lett. **124**, 120403 (2020).